ELSEVIER

Chemical Geology 203 (2004) 139–151

CHEMICAL GEOLOGY
INCLUDING
ISOTOPE GEOSCIENCE

www.elsevier.com/locate/chemgeo

Co-precipitation of Sr^{2+} and Ba^{2+} with aragonite by membrane diffusion of CO$_2$ between 10 and 50 °C[☆]

M. Dietzel[a,*], N. Gussone[b], A. Eisenhauer[b]

[a] Institute of Engineering Geology and Applied Mineralogy, Graz University of Technology, Rechbauerstrasse 12, A-8010 Graz, Austria
[b] Geomar, Forschungszentrum für Marine Geowissenschaften, Wischhofstr. 1-3, 24148 Kiel, Germany

Received 11 June 2002; accepted 19 September 2003

Abstract

Aragonite is precipitated by a new CO$_2$-diffusion technique from a Ca^{2+}–Mg^{2+}–Cl^- solution between 10 and 50 °C. Crystallisation of aragonite instead of calcite occurs by maintaining a [Mg^{2+}]/[Ca^{2+}] ratio of 2 in the fluid. The dissolved inorganic carbon (DIC) is received by diffusion of CO$_2$ through a polyethylene membrane (diffusion coefficient: $D_{CO_2} = 10^{-6.4}$ cm^2 s^{-1} at 19 °C). It is suggested that significant amounts of DIC may be transferred by diffusion of CO$_2$ in natural systems if the CO$_2$ gradient is high. The CO$_2$-diffusion technique is used as a kind of simple mixed flow reactor for the co-precipitation of barium and strontium with aragonite. The distribution coefficients of Ba^{2+} and Sr^{2+} decrease from 10 to 50 °C according to $D^*_{Ba,a} = 2.42 - 0.03595T$ (°C) and $D^*_{Sr,a} = 1.32 - 0.005091T$ (°C). At 25 °C, the distribution coefficients are $D^*_{Ba,a} = 1.5 \pm 0.1$ and $D^*_{Sr,a} = 1.19 \pm 0.03$. The effect of temperature on $D^*_{Ba,a}$ is about one order of magnitude higher versus that on $D^*_{Sr,a}$. Thus, Ba^{2+} may be a potential paleotemperature indicator if the composition of the solution is known.

Keywords: Aragonite; CO$_2$ diffusion; Co-precipitation; Barium; Strontium

1. Introduction

In natural environments near the Earth's surface, calcium carbonate minerals occur as precipitates from aqueous solutions. Their precipitation requires the availability of calcium and carbonate ions. Dissolved calcium ions are primarily gained by the dissolution of minerals and rocks (e.g. silicates and carbonates). Potential sources of carbonate ions are carbonate minerals by dissolution, organic matter by biochemical decomposition, atmospheric carbon dioxide and CO$_2$ of volcanic origin.

Transport of dissolved inorganic carbon (DIC) and calcium can be due to hydrodynamic processes. If the flow behaviour is negligible, aqueous component transport may be induced by diffusion either in the interstitial fluid or through micropores, faults, interfaces of the solids or various kinds of geomembranes (e.g. McBride, 1994). Potential natural membranes are layers of clay minerals, deposits of silica and Al/Fe-hydroxide gels, accumulations of degraded organic matter or semi-permeable cell membranes, whereas anthropogenic geomembranes consist of synthetic polymers, which are worldwide

---

[☆] Supplementary data associated with this article can be found, in the online version, at doi:10.1016/j.chemgeo.2003.09.008.

[*] Corresponding author. Tel.: +43-316-873-6360; fax: +43-316-873-6861.

E-mail address: dietzel@egam.tu-graz.ac.at (M. Dietzel).

doi:10.1016/j.chemgeo.2003.09.008

used for applications of solid waste disposal, municipal water, wastewater, the aquaculture industry, etc. (Jost, 1972; Unger, 1984; Fukuoka, 1994; Bradley et al., 2001).

In the present study, CO_2 diffusion through a polyethylene membrane induces a CO_2 flux to crystallize aragonite from an aqueous solution. The applied CO_2-diffusion technique is used as a simple mixed flow reactor where the CO_2 flux may be easily varied by changing the thickness or type of the membrane, or by adjusting the chemical composition of the solution (e.g. pH, HCO_3^- or Ca^{2+} concentration). A similar technique was formerly applied by Dietzel and Usdowski (1996) for co-precipitation of Sr^{2+} with calcite. Moreover, diffusion techniques have been used for years for crystallizing carbonate minerals by counter-diffusion of reactants through gels (e.g. Henisch, 1970; Prieto et al., 1997). The growth of carbonate minerals by counter-diffusion appears within a gel, whereas by CO_2-diffusion technique aragonite crystallizes from an aqueous solution.

The crystallisation of aragonite by CO_2-diffusion technique is used to investigate the co-precipitation of strontium and barium with aragonite. The literature dealing with incorporation of Sr^{2+} into the polymorphs aragonite and calcite is voluminous (aragonite: e.g. Kinsman and Holland, 1969; Kitano et al., 1971; Usdowski, 1973; Smith et al., 1979; Plummer and Busenberg, 1987; Plummer et al., 1992; De Villiers et al., 1994; Casey et al., 1996; calcite: e.g. Katz et al., 1972; Lorens, 1981; Mucci and Morse, 1983; Pingitore and Eastman, 1986; Tesoriero and Pankow, 1996; Rimstidt et al., 1998; Lea et al., 1999; Rickaby and Schrag, 2002). Studies with respect to the co-precipitation of Ba^{2+} with aragonite and calcite are rather scarce (aragonite: e.g. Kitano et al., 1971; Bath et al., 2000; calcite: e.g. Tesoriero and Pankow, 1996; Pingitore, 1986; Kitano et al., 1973; Rimstidt et al., 1998). The above studies show that the incorporation of Sr^{2+} and Ba^{2+} into aragonite is about two orders of magnitude higher than into calcite (Kinsman and Holland, 1969; Lorens, 1981; Tesoriero and Pankow, 1996; Kitano et al., 1971). Differences between these elements can be explained by the ionic radii of Sr^{2+} and Ba^{2+} and the specific crystal structure of the polymorphs.

In principle, strontium ($Me^{2+}=Sr^{2+}$) and barium ($Me^{2+}=Ba^{2+}$) are incorporated into aragonite according to the general reaction

$$x\mathrm{Ca}^{2+} + (1-x)\mathrm{Me}^{2+} + \mathrm{CO}_3^{2-} = \mathrm{Ca}_x\mathrm{Me}_{(1-x)}\mathrm{CO}_3 \tag{1}$$

The related distribution coefficient is defined according to the equation

$$D_{\mathrm{Me,a}} = \frac{X_{\mathrm{MeCO_3}}/X_{\mathrm{CaCO_3}}}{[\mathrm{Me}^{2+}]/[\mathrm{Ca}^{2+}]} \tag{2}$$

by the mole fractions $X_{\mathrm{MeCO_3}}$ and $X_{\mathrm{CaCO_3}}$ of aragonite and the molar concentrations $[Me^{2+}]$ and $[Ca^{2+}]$ of the aqueous solution. The distribution coefficient may be related to the activities of dissolved components according to

$$D^*_{\mathrm{Me,a}} = \frac{X_{\mathrm{MeCO_3}}/X_{\mathrm{CaCO_3}}}{\{\mathrm{Me}^{2+}\}/\{\mathrm{Ca}^{2+}\}} \tag{3}$$

where $\{Ca^{2+}\}$ and $\{Me^{2+}\}$ denote activities of Ca^{2+} and trace component Me^{2+} in the solutions. The activities are obtained by the concentrations, $[X]$, and activity coefficients, γ_x, of the respective dissolved component X according to $\{X\}=[X]\cdot\gamma_x$.

2. Methods

In Fig. 1, the experimental set up for the crystallisation of aragonite is shown. A 500-ml polyethylene bottle (wall thickness: 0.2 cm) containing 35 g solid $NaHCO_3$ was filled with double distilled water (inner solution). This solution was saturated with CO_2 gas from a tank at 1 atm. The sodium bicarbonate was completely dissolved within 1 h. The time to achieve chemical equilibrium was monitored by measuring pH. At equilibrium, the pH is 7.5.

The closed bottle containing the inner solution was placed into a vessel containing 5 l of the outer solution. The outer solution consists of $[Ca^{2+}]=0.01$ mol kg^{-1}, $[Mg^{2+}]=0.02$ mol kg^{-1} and $[Cl^-]=0.06$ mol kg^{-1} (formed by dissolution of solid $CaCl_2\cdot 2H_2O$ and $MgCl_2\cdot 6H_2O$) and was kept under nitrogen atmosphere to prevent absorption of atmospheric

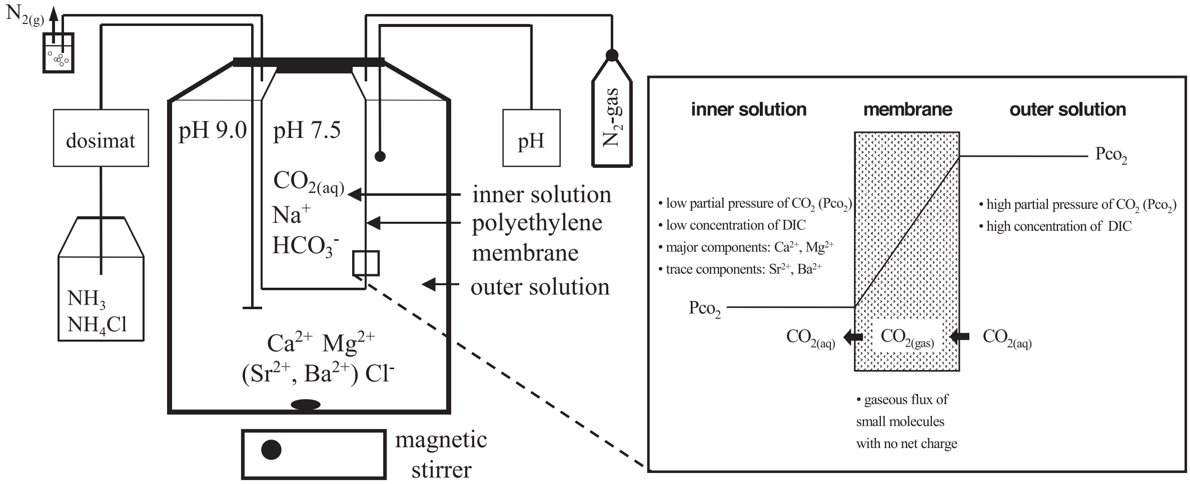

Fig. 1. Experimental set up for the crystallisation of aragonite and the co-precipitation of strontium and barium with aragonite by CO_2 diffusion through a polyethylene membrane. The transferred CO_2 reacts with dissolved Ca^{2+} to form aragonite according to Eq. (4).

CO_2. A pH of 9.0 was fixed in the outer solution by the addition of a freshly prepared ammonia buffer during each experimental run. At this pH, the solution becomes undersaturated with respect to brucite. The buffer concentration of the outer solution was about 10^{-3} mol l^{-1} of NH_3. In all experiments, reagent grade chemicals (p.a. Merck) and pure gas (Messer Griesheim, CO_2: 99.995 Vol%) were used.

As the experiments proceed, CO_2 diffuses from the inner solution through the polyethylene membrane into the outer solution. Consequently, aragonite crystallises in the continuously stirred outer solution. The temperature was kept constant with a temperature controlled water bath (± 0.3 °C; Julabo HC E07 F18). Samples of the outer solution (50 ml) were removed with a plastic syringe. In the filtrated outer solutions (0.2 μm, Sartorius 11309) and the inner solutions, the concentrations of Ca^{2+}, Mg^{2+}, Sr^{2+} and Na^+ were analysed by inductively coupled plasma optical emission spectroscopy with an analytical error of about 1% (ICP-OES, Perkin Elmer Optima 3300DV). For simultaneous ICP-OES analyses, the uncertainty with respect to the $[Sr^{2+}]/[Ca^{2+}]$ and $[Ba^{2+}]/[Ca^{2+}]$ ratios is $< 1\%$, as determined by repeated analysis of samples and standards. As two analysed ratios have to be considered for the calculation of the distribution coefficients (see Eq. (2)) error propagation yields in an uncertainty of 2% for the values of $D_{Me,a}$. In several experiments, HCO_3^- concentrations were analysed by titration with 0.01*n* hydrochloric acid with an analytical error of about 4% to follow CO_2 diffusion and aragonite precipitation.

To maintain an almost constant composition of the outer solution for the co-precipitation of Sr^{2+} and Ba^{2+} with aragonite not more than 100 mg aragonite has to be formed. The time periods for the deposition of 100 mg aragonite were determined by analysing calcium concentration. The amount of about 0.001 mol Ca^{2+} (100 mg aragonite) contained in the

Table 1
Composition of the outer solutions and the respective precipitated solids

$[Ca^{2+}]$	$[Mg^{2+}]$	pH	Solid	*T* (°C)
0.1	–	10.4	calcite	19
0.1	0.001	10.4	calcite	19
0.1	0.005	10.4	calcite	19
0.1	0.01	10.4	aragonite + calcite	19
0.1	0.02	10.4	aragonite + calcite	19
0.1	0.05	10.4	aragonite + calcite	19
0.1	0.1	10.4	aragonite + brucite	19
0.1	0.1	9.0	aragonite + brucite	19
0.01	0.01	9.0	aragonite	19–50
0.01	0.02	9.0	aragonite	10–50

Concentrations are given in mol kg^{-1}.

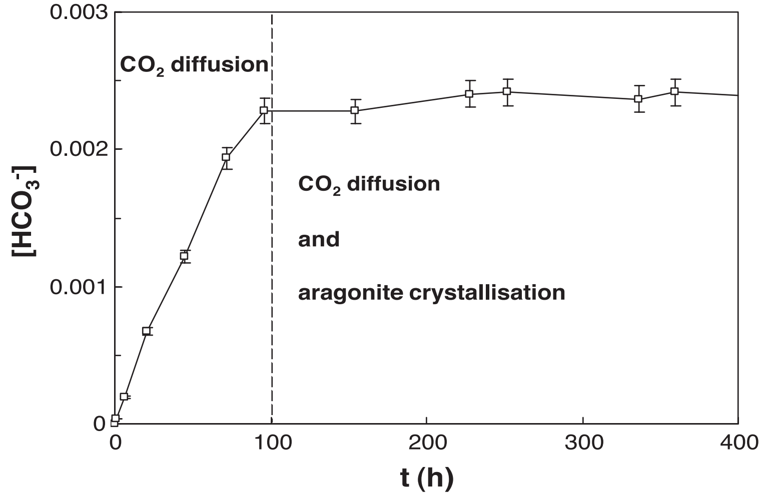

Fig. 2. Bicarbonate concentration of the outer solution as a function of reaction time (19 °C; Table 2).

precipitated aragonite from each run represents only 2 mol% of the initial amount of 0.05 mol Ca^{2+} in the outer solution (5 l). Moreover, Sr^{2+} and Ba^{2+} concentrations decrease by the same order of magnitude due to the value of $D_{Ba,a}$ and $D_{Sr,a}$ being close to one (Eq. (2)). Thus, the analysed $[Sr^{2+}]/[Ca^{2+}]$ and $[Ba^{2+}]/[Ca^{2+}]$ ratios of the outer solution are virtually constant during the experiments. The calculation of activities and aqueous speciation for all experiments were performed using the program SOLMINEQ88 (Kharaka et al., 1988) considering ion-pairing.

At the end of each co-precipitation experiment, the precipitated solids were removed from the outer solution by filtration through a 0.2-μm membrane filter under a nitrogen atmosphere. Some additional solids were mechanically removed from the walls of the 500-ml bottle. The solids were washed with double distilled water until the remaining solution was chloride free (as checked by the addition of $AgNO_3$), freeze dried and weighed. The precipitated aragonite was dissolved in diluted hydrochloric acid (6 wt.%) and the concentrations of Ca^{2+}, Mg^{2+} and Sr^{2+} were analysed by ICP-OES.[1]

If the amount of aragonite exceeded 110 mg, the respective experiment was discarded. In each experiment, the formation of aragonite was confirmed by X-ray diffraction (XRD; goniometer type Philips PW 1130/1370) and infrared spectroscopy (FTIR; Perkin Elmer 1600). XRD (3.035 Å reflex) and FTIR analyses (876 cm^{-1} vibration) provide detection limits of 5 and 2 wt.% calcite in the presence of aragonite, as confirmed by analyses of prepared calcite–aragonite mixtures with well know composition. Moreover, analyses of the precipitates by optical microscopy (Leica DMLP) were carried out. Calcite crystals show always rhombohedral habit, whereas aragonites occur as fibrous crystals.

Obviously, the values of distribution coefficients are most sensitive on aragonite versus calcite formation. Although individual calcite crystals can be identified by microscopy, which significantly improves the detection limit of 2% for aragonite, a respective percentage is not easy to predict. As a worst case, calcite may be formed in the presence of aragonite at a proportion of 2%. For example, $D^{*}_{Sr,a} = 1.19$ (present study) and $D_{Sr,calcite} = 0.021$ (Tesoriero and Pankow, 1996) at 25 °C. The $D^{*}_{Sr,a}$ value decreases down to 1.17 as both calcite and aragonite are formed at a ratio of 2:98. Such deviation is within the range of the accuracy of $D^{*}_{Sr,a}$.

---

[1] Analytical data are provided by an excel-file via Science Direct at doi:10.1016/j.chemgeo.2003.09.008.

3. Formation of aragonite versus calcite

The precipitation of calcite or aragonite induced by diffusion of CO_2 can be expressed by the equation

$$Ca^{2+} + CO_2 + OH^- = CaCO_3 + H^+ \quad (4)$$

At low temperatures of sedimentary environments, calcite is the stable polymorph of $CaCO_3$ and may be easily precipitated from aqueous solutions, whereas inorganic precipitation of aragonite is preferentially obtained at elevated temperatures and in solutions containing magnesium chloride (e.g. Berner, 1966; Kinsman and Holland, 1969; Kitano et al., 1971; Usdowski, 1973; Zhou and Zheng, 2001). Therefore, several experiments were carried out to determine the outer solution compositions that would yield aragonite as the sole reaction product.

The first set of experimental runs was carried out at a temperature of 19 °C, pH 10.4, 0.1 mol kg^{-1} of Ca^{2+} and magnesium concentrations between 0.001 and 0.1 mol kg^{-1} of Mg^{2+} (Table 1). At a $[Mg^{2+}]/[Ca^{2+}]$ ratio of 1, the crystallisation of calcite was completely inhibited, but brucite precipitated. To avoid brucite formation, the pH was kept at 9.0 and the Mg^{2+} concentration was adjusted to 0.01 mol kg^{-1} at a $[Mg^{2+}]/[Ca^{2+}]$ ratio of 1. This was checked by chemical analyses of the Mg^{2+} content of the dissolved solids (ICP-OES). Under these conditions, aragonite precipitated as sole reaction product. The formation of aragonite was confirmed by X-ray diffraction and FTIR analyses. In any case, the absence of rhombohedral calcite crystals was also verified by microscopy. Same results were obtained up to temperatures of 50 °C, whereas twice as much Mg^{2+} was required to inhibit the formation of calcite at 10 °C. Experiments without Ca^{2+} but with 0.02 mol kg^{-1} of Mg^{2+} and Me^{2+} used for the co-precipitation experiments show that no precipitation of any additional solid occurs within the respective range of temperature and reaction

Table 2
Concentration of HCO_3^- (mmol l^{-1}) of the outer solution and the obtained diffusion coefficient, D_{CO_2} (cm s^{-1}), of CO_2 through the polyethylene membrane (19 °C) as a function of reaction time t

t (h)	$[HCO_3^-]$	N_{CO_2}	log D_{CO_2}
1	0.0344	0.000172	− 6.34
6	0.197	0.000982	− 6.36
21	0.675	0.003376	− 6.37
45	1.22	0.006101	− 6.44
72	1.93	0.009672	− 6.45
96	2.28	0.011385	− 6.51

N_{CO_2}: moles CO_2 released by diffusion.

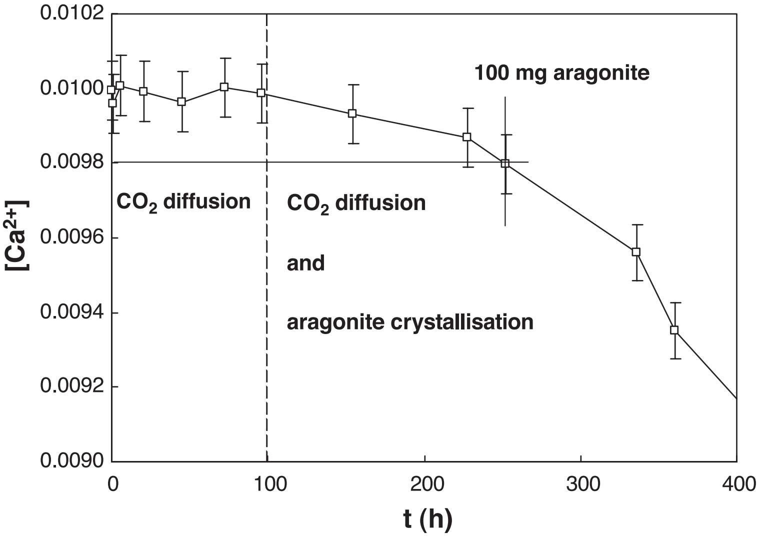

Fig. 3. Calcium concentration of the outer solution as a function of reaction time (19 °C). A decrease down to 0.0098 mol l^{-1} of Ca^{2+} at 250 h reaction time represents precipitation of 100 mg aragonite.

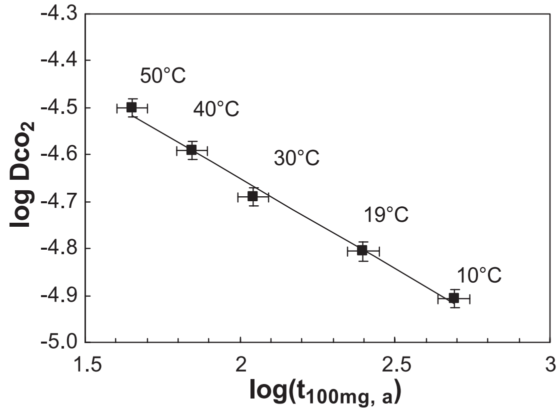

Fig. 4. Diffusion coefficient of $CO_{2(aq)}$ in water ($cm^2\ s^{-1}$) versus time (h) to precipitate 100 mg aragonite (D_{CO_2}-values were taken from Unver and Himmelblau, 1964).

times. Thus, all co-precipitation experiments were carried out at pH 9.0, a $[Mg^{2+}]/[Ca^{2+}]$ ratio of 2 and 0.01 mol kg^{-1} of Ca^{2+}.

4. Diffusion of CO_2 and precipitation of aragonite

In Fig. 1, the requirements for a flux of DIC from the inner to the outer solution and the precipitation of aragonite by CO_2 diffusion through a membrane are schematically shown. The CO_2 diffusion is controlled by the CO_2 gradient of the partial pressure, which is kept constant by the high concentration of DIC of the inner solution and the constant pH of the outer solution. It was confirmed by chemical analyses of the inner and outer solutions that none of the dissolved ions enters the polyethylene membrane during the experimental run. As the diffusion of negatively charged carbonate species requires a simultaneous diffusion of corresponding cations, it is concluded that the CO_2 molecules diffuse through the membrane with no net charge transfer. Consequently, no significant DIC transfer occurs if the inner solution contains sodium bicarbonate without the addition of gaseous CO_2.

In Figs. 2 and 3, the typical evolution of bicarbonate and calcium concentrations of the outer solution is shown for 19 °C as the reaction proceeds. Bicarbonate concentration increases up to a reaction time of about 100 h (Fig. 2). At this stage, aragonite crystallises which is shown by a decrease of Ca^{2+} concentration (Fig. 3). The concentration of HCO_3^- in the outer solution analysed as aragonite precipitation occurs is 0.0301, 0.0227, 0.00108, 0.000713 and 0.000524 mol l^{-1} of HCO_3^- for 10, 19, 30, 40 and 50 °C, respectively. The calculated saturation indices for aragonite

Table 3
Co-precipitation of Ba^{2+} with aragonite

T (°C)	$[Mg^{2+}]/[Ca^{2+}]$	X_{MgCO_3}/X_{CaCO_3}	$[Ba^{2+}]/[Ca^{2+}]$	X_{BaCO_3}/X_{CaCO_3}	$D_{Ba,a}$	$\{Ba^{2+}\}/\{Ca^{2+}\}$	$D^*_{Ba,a}$
10	2.05	0.000836	0.0009515	0.001727	1.815	0.0009103	1.897
10	2.07	0.000622	0.00009485	0.0001862	1.963	0.00009070	2.053
10	2.07	0.000367	0.00009485	0.0001863	1.964	0.00009070	2.054
19	2.00	0.000352	0.0009586	0.001779	1.856	0.0009145	1.945
30	2.08	0.002197	0.002961	0.004302	1.453	0.002818	1.527
30	2.04	0.000976	0.0009968	0.001333	1.337	0.0009464	1.408
30	2.02	0.001232	0.0002976	0.0003375	1.134	0.0002830	1.193
30	2.07	0.001344	0.00009972	0.0001354	1.358	0.00009463	1.431
40	2.04	0.000492	0.003075	0.002716	0.883	0.002913	0.932
40	1.96	0.001043	0.0003310	0.0002322	0.701	0.0003140	0.739
40	1.96	0.000108	0.0001034	0.00008085	0.782	0.00009746	0.830
50	1.98	0.000628	0.003018	0.002068	0.685	0.002860	0.723
50	2.00	0.000389	0.001026	0.0005130	0.500	0.0009687	0.530
50	2.01	0.001362	0.0003118	0.0001918	0.615	0.0002949	0.650
50	2.04	0.000489	0.0001042	0.00007248	0.696	0.00009834	0.737

Ratios of molar concentrations, [ ], and activities, { }, of the components in the outer solution, and ratios of mol fractions in the aragonite, X_{MeCO_3}. $D_{Ba,a}$ and $D^*_{Ba,a}$ denote the distribution coefficients of Ba^{2+} in aragonite considering molar concentration and activities of dissolved components, respectively.

($SI_{aragonite}$ = log(ion activity product/solubility product); solubility product from Plummer and Busenberg, 1982) are 1.5, 1.4, 1.2, 1.1 and 1.0, respectively, which shows supersaturation with respect to aragonite in any experimental solution.

Prior to the onset of aragonite precipitation, the CO_2 diffusion through the membrane is expressed by

$$\frac{\mathrm{d}N_{CO_2}}{F\cdot \mathrm{d}t} = D_{CO_2}\frac{[CO_{2(aq)}]_{in} - [CO_{2(aq)}]_{out}}{\Delta x} \qquad (5)$$

N_{CO_2} is the number of moles CO_2 diffused, F is the surface area of the polyethylene bottle (340 cm^2), D_{CO_2} is the diffusion coefficient and t is time. $[CO_{2(aq)}]_{in}$ and $[CO_{2(aq)}]_{out}$ represent the aqueous CO_2 concentration of the inner and outer solutions, respectively. Δx denotes the polyethylene membrane thickness (0.2 cm).

The CO_2 concentration of the inner solution is given by the concentration of sodium ions at pH 7.5. The addition of 70 g l^{-1} of $NaHCO_3$ results in 0.833 mol l^{-1} of Na^+. At pH 7.5, the concentration of bicarbonate is almost equivalent to that of sodium ($[HCO_3^-] \approx [Na^+]$). Thus, a value of $[CO_{2(aq)}]_{in}$ of about $10^{-4.2}$ mol cm^{-3} is obtained ($[H_2CO_3^*]=[H^+]\cdot[HCO_3^-]\cdot K_1^{-1}$, $[H_2CO_3^*]=[CO_{2(aq)}]+[H_2CO_3]$

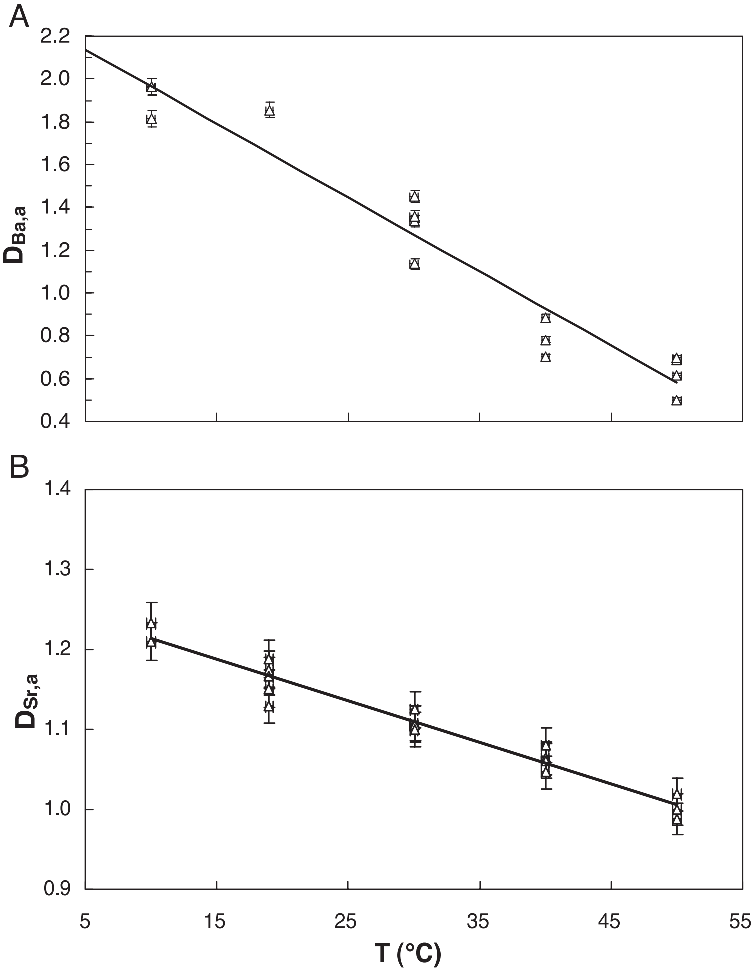

Fig. 5. Distribution coefficient of Ba^{2+} (A) and Sr^{2+} (B) with respect to aragonite as a function of temperature (see Eq. (2)). Regression lines: $D_{Ba,a} = 2.31 - 0.03455T$ (°C), correlation coefficient: 0.942; $D_{Sr,a} = 1.27 - 0.005212T$ (°C), correlation coefficient: 0.953.

and $[CO_{2(aq)}] \gg [H_2CO_3]$; K_1: first dissociation constant of carbonic acid, $\log K_1 = 10^{-6.39}$ at 19 °C from Harned and Davis, 1943). Values of $[CO_{2(aq)}]_{out}$ are in the range from 10^{-8} to 10^{-10} mol cm^{-3} for the HCO_3^- concentrations in Table 2 at pH 9.0. Thus, $[CO_{2(aq)}]_{in} - [CO_{2(aq)}]_{out} \approx [CO_{2(aq)}]_{in}$.

If no aragonite formation occurs the number of moles CO_2, N_{CO_2}, gained by the diffusion equals the total number of moles DIC in the outer solution. Considering the above values and Eq. (5), a mean value of the diffusion coefficient $D_{CO_2} = 10^{-6.4}$ cm^2 s^{-1} is obtained (Table 2), which is about two orders of magnitudes lower than the value of the diffusion coefficient of CO_2 in aqueous solution (D_{CO_2}(in water)$= 10^{-4.7}$ cm^2 s^{-1}; Unver and Himmelblau, 1964).

Aragonite crystallisation reduces the Ca^{2+} concentration in the outer solution (Fig. 2). The results show that aragonite begins to precipitate within 100 h of the onset of the experiments. After a reaction time of about 250 h, 100 mg aragonite precipitates. The reaction times for the deposition of 100 mg

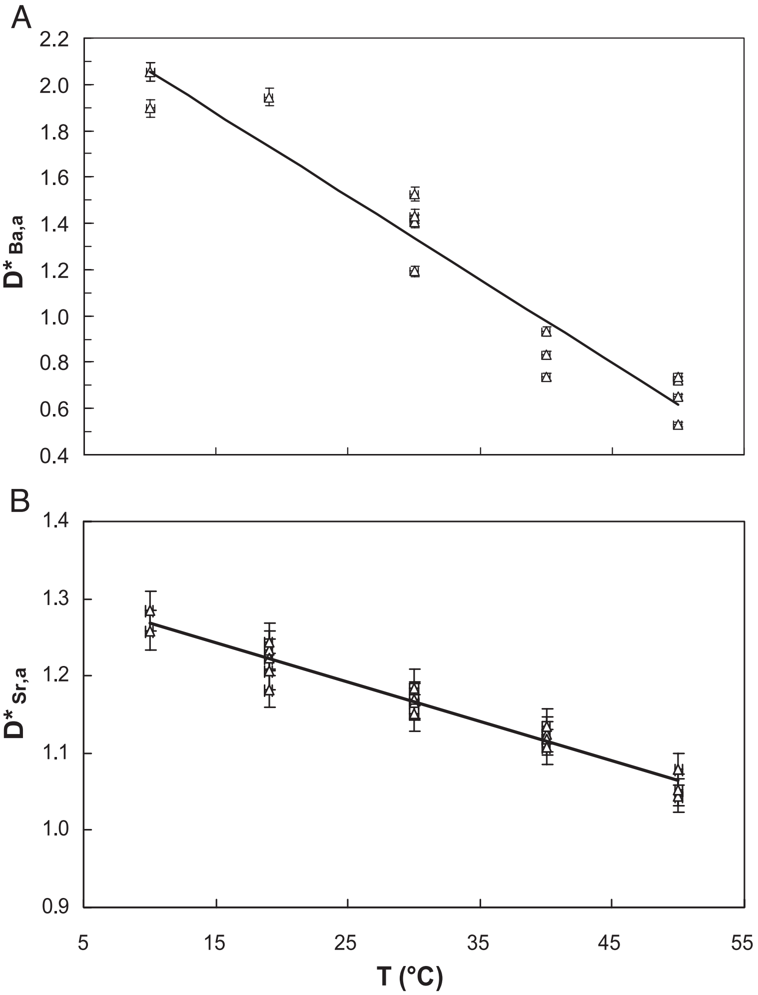

Fig. 6. Activity-corrected distribution coefficient of Ba^{2+} (A) and Sr^{2+} (B) with respect to aragonite as a function of temperature (see Eq. (3)). Regression lines: $D_{Ba,a}* = 2.42 - 0.03595T$ (°C), correlation coefficient: 0.940; $D_{Sr,a}* = 1.32 - 0.005091T$ (°C), correlation coefficient: 0.945.

aragonite ($t_{100\ \mathrm{mg,a}}$, required for co-precipitation experiments) for 10, 19, 30, 40 and 50 °C are about 490, 250, 110, 70 and 45 h, respectively. In principle, the value of $t_{100\ \mathrm{mg,a}}$ strongly depends on the CO_2 diffusion coefficient of the polyethylene membrane, which varies with temperature. This correlation may be followed in Fig. 4 by $t_{100\ \mathrm{mg,a}}$ versus the value for the diffusion coefficient of CO_2 in water. Moreover, the temperature dependence of the reaction time $t_{100\ \mathrm{mg,a}}$ is affected by the decrease of the solubility of aragonite at elevated temperatures (see Plummer and Busenberg, 1982). Although there is no control on the aragonite surface area in the reactor an approximation of the aragonite precipitation rates R referred to half of total aragonite formation yields R-values in the range from 10^{-11} up to 10^{-10} mol mg^{-1} s^{-1} for 10–50 °C.

5. Co-precipitation of barium and strontium with aragonite

Fifteen barium co-precipitation experiments were carried out between 10 and 50 °C. The results in Table 3 indicate that the distribution coefficient of barium into aragonite does not depend on the $[Ba^{2+}]/[Ca^{2+}]$ ratio, consistent with the validity of the distribution law of Eq. (2).

Figs. 5 and 6 show the variation of the distribution coefficient $D_{\mathrm{Ba,a}}$ and $D^*_{\mathrm{Ba,a}}$ as a function of temperature (see Eqs. (2) and (3), respectively). The value of $D_{\mathrm{Ba,a}}$ decreases as the temperature increases according to the equation

$$D_{\mathrm{Ba,a}} = 2.31 - 0.03455T(^\circ\mathrm{C}) \tag{6}$$

If the activities of Ca^{2+} and Ba^{2+} in the solutions are considered the expression

$$D^*_{\mathrm{Ba,a}} = 2.42 - 0.03595T(^\circ\mathrm{C}) \tag{7}$$

is obtained. The range of distribution coefficients given by Kitano et al. (1971) for the incorporation of barium into aragonite for 20 °C is in agreement with the results of the present study.

The results of 18 strontium co-precipitation experiments are presented in Table 4. Like Ba^{2+}, the

Table 4
Co-precipitation of Sr^{2+} with aragonite

T (°C)	$[Mg^{2+}]/[Ca^{2+}]$	X_{MgCO_3}/X_{CaCO_3}	$[Sr^{2+}]/[Ca^{2+}]$	X_{SrCO_3}/X_{CaCO_3}	$D_{\mathrm{Sr,a}}$	$\{Sr^{2+}\}/\{Ca^{2+}\}$	$D^*_{\mathrm{Sr,a}}$
10	1.96	0.001115	0.0300	0.03701	1.234	0.02882	1.284
10	2.00	0.000322	0.0100	0.01210	1.210	0.009609	1.259
19	1.99	0.004476	0.0300	0.03391	1.130	0.02868	1.182
19	1.81	0.005073	0.01653	0.01902	1.151	0.01577	1.206
19	1.85	0.000367	0.002190	0.002574	1.175	0.002088	1.233
19	1.86	0.000653	0.001653	0.001928	1.166	0.001575	1.224
19	1.81	0.000723	0.0005510	0.0006545	1.188	0.0005260	1.244
30	2.00	0.000518	0.0300	0.03323	1.108	0.02849	1.166
30	2.00	0.000363	0.0100	0.01125	1.125	0.009503	1.184
30	2.00	0.000438	0.00300	0.003320	1.107	0.002841	1.169
30	1.95	0.000289	0.00100	0.001100	1.100	0.0009547	1.152
40	2.02	0.000570	0.0300	0.03192	1.064	0.02841	1.124
40	1.98	0.000484	0.0100	0.01061	1.061	0.009481	1.119
40	1.99	0.000463	0.00300	0.003140	1.047	0.002834	1.108
40	1.98	0.000912	0.00100	0.001080	1.080	0.0009522	1.134
50	1.97	0.000896	0.0300	0.03057	1.019	0.02833	1.079
50	2.02	0.000952	0.0100	0.009890	0.989	0.009462	1.045
50	1.96	0.005901	0.00100	0.00100	1.000	0.0009506	1.052

Ratios of molar concentrations, [ ], and activities, { }, of the components in the outer solution, and ratios of mol fractions in the aragonite, X_{MeCO_3}. $D_{\mathrm{Sr,a}}$ and $D^*_{\mathrm{Sr,a}}$ denote the distribution coefficients of Sr^{2+} in aragonite considering molar concentration and activities of dissolved components, respectively.

incorporation of Sr^{2+} into aragonite follows the Eq. (2). The values of the distribution coefficients $D_{Sr,a}$ and $D^{*}_{Sr,a}$ decrease with increasing temperature from 10 to 50 °C according to the equation

$$D_{Sr,a} = 1.27 - 0.005212T(^{\circ}C) \tag{8}$$

and

$$D^{*}_{Sr,a} = 1.32 - 0.005091T(^{\circ}C) \tag{9}$$

In Fig. 7, the expression 8 is extrapolated to elevated temperatures and plotted versus the results obtained by Kinsman and Holland (1969). They studied the co-precipitation of Sr^{2+} with aragonite in seawater between 16 and 96 °C. Their results are quite similar to those of the present study. The Ca^{2+} concentrations of the experimental solutions in the present study are almost identical to that of seawater ($[Ca^{2+}] = 0.010$ mol kg^{-1}), whereas seawater contains additional magnesium and chloride as well as high sodium and sulfate concentrations (seawater: $[Mg^{2+}] = 0.053$, $[Cl^{-}] = 0.55$, $[Na^{+}] = 0.47$ and $[SO_4^{2-}] = 0.028$ mol kg^{-1}; Culkin, 1967). Thus, it is concluded that the value of $D_{Sr,a}$ is almost constant in the range of the chemical composition of the present experimental solutions ($[Mg^{2+}] = 0.02$ and $[Cl^{-}] =$ 0.06 mol kg^{-1}) and the seawater. It is implied from the co-precipitation experiments of Holland et al. (1963) at 96 °C that the presence of sulfate ions may cause lower $D_{Sr,a}$ values (Fig. 7). This is not confirmed in the present study up to a temperature of 50 °C.

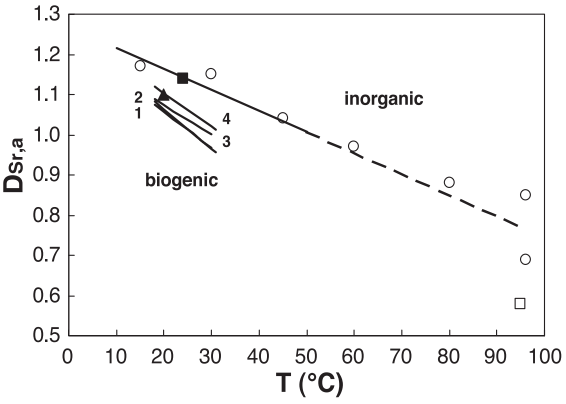

Fig. 7. Distribution coefficient of Sr^{2+} for inorganic and biogenic induced aragonite precipitation as a function of temperature. Inorganic: (○) Kinsman and Holland (1969), (■) Joschi (1960), (□) Holland et al. (1963), (▲) Kitano et al. (1971), (solid line) present study (according to Eq. (8)); biogenic: (1) De Villiers et al. (1995), (2) Weber (1973), (3) Beck et al. (1992), (4) Smith et al. (1979).

Fig. 7 shows that the incorporation of Sr^{2+} into aragonite is different if the precipitation is induced by biotic processes which may be related to the so called "vital effects" (e.g. Weber, 1973; Smith et al., 1979; Beck et al., 1992; De Villiers et al., 1995). Nevertheless, the variation of $D_{Sr,a}$ with temperature is similar to that for the inorganic precipitation of aragonite.

6. Conclusion

The applied CO_2-diffusion technique provides a simple mixed flow reactor for precipitation of aragonite by a CO_2 flux through a membrane. The co-precipitation experiments show that the incorporation of Ba^{2+} and Sr^{2+} into aragonite depends on the respective Me^{2+} to Ca^{2+} ratio of the solution according to Eqs. (2) and (3), and decreases as the temperature increases from 10 to 50 °C.

The experimentally obtained distribution coefficients may be compared to theoretical distribution coefficients at thermodynamic equilibrium $K_{Me,a}$. The values of $K_{Me,a}$ are related to the activities of $CaCO_{3(s)}$ and $MeCO_{3(s)}$ in the aragonite (a_{CaCO_3} and a_{MeCO_3}, respectively) and to the activities of the dissolved cations according to

$$K_{Me,a} = \frac{a_{MeCO_3}/a_{CaCO_3}}{\{Me^{2+}\}/\{Ca^{2+}\}} = \frac{X_{MeCO_3}/X_{CaCO_3}}{\{Me^{2+}\}/\{Ca^{2+}\}} \cdot \zeta_{MeCO_3}/\zeta_{CaCO_3} \tag{10}$$

where ζ_{CaCO_3} and ζ_{MeCO_3} denote the activity coefficients of $CaCO_{3(s)}$ and $MeCO_{3(s)}$ in the aragonite, respectively. The activity of Ca^{2+} and Me^{2+} in the solutions can be calculated and the activity of the carrier component Ca^{2+} in aragonite is well approximated as being equal to unity as X_{MeCO_3} is low (e.g. Morse and Mackenzie, 1990). The space group of aragonite, strontianite and witherite is *Pmcn*. In any crystal lattice of such orthorhombic carbonates divalent metal ions are coordinated to nine oxygen. In this case, the theoretical value of $K_{\mathrm{Me,a}}$ for co-precipitation of Sr^{2+} and Ba^{2+} with aragonite may be approximated by the respective solubility products according to

$$K_{\mathrm{Me,a}} = \frac{K_{\mathrm{CaCO_3}}}{K_{\mathrm{MeCO_3}}} \tag{11}$$

(e.g. Böttcher, 1997). Individual values for the solubility products $K_{\mathrm{CaCO_3}}$, $K_{\mathrm{SrCO_3}}$ and $K_{\mathrm{BaCO_3}}$ for aragonite, strontianite and witherite are given by Plummer and Busenberg (1982) and Busenberg and Plummer (1984, 1986), respectively. The calculated values of the distribution coefficients at thermodynamic equilibrium $K_{\mathrm{Sr,a}}$ and $K_{\mathrm{Ba,a}}$ decreases from 10.8 to 6.8 and 2.4 to 1.2 as the temperature increases from 10 to 50 °C, respectively.

If the activity-corrected distribution coefficient, $D^*_{\mathrm{Me,a}}$, represents distribution at thermodynamic equilibrium, the activity coefficients of $\zeta_{\mathrm{MeCO_3}}$ in aragonite may be obtained according to the equation

$$D^*_{\mathrm{Me,a}} = \frac{K_{\mathrm{Me,a}}}{\zeta_{\mathrm{MeCO_3}}} \tag{12}$$

The results in Fig. 6 show that $D^*_{\mathrm{Me,a}} < K_{\mathrm{Me,a}}$ in any case, which may indicate $\zeta_{\mathrm{MeCO_3}} > 1$ under the assumption of thermodynamic equilibrium.

In the present experiments, aragonite crystallizes spontaneously. The approximation of respective precipitation rates yields low values compared to other co-precipitation studies (e.g. Lorens, 1981; Tesoriero and Pankow, 1996). Obviously, at low precipitation rates, equilibrium of trace element distribution between carbonate minerals and aqueous solutions may be reached rather than at high rates. Nevertheless, aragonite formation by CO_2 diffusion technique is controlled by the flux of CO_2 into a Ca^{2+} containing solution. Although, the overall precipitation rate which is approximated by the total amount of aragonite formation is low, the kinetics for aragonite crystallisation according to Eq. (4) may be significantly faster. Further investigations have to be carried out to verify the effect of precipitation kinetics and flux of CO_2 on the values of respective distribution coefficients. This may be done by changing the chemical composition of the solution or the type of membrane.

The measured and theoretical distribution coefficients, $D^*_{\mathrm{Me,a}}$ and $K_{\mathrm{Me,a}}$, decrease as the temperature increases for both barium and strontium co-precipitation with aragonite. Nevertheless, the effect of temperature on $D^*_{\mathrm{Ba,a}}$ is almost one order of magnitude higher for barium than that for strontium (Eqs. (7) and (9)). Thus, the Ba^{2+} content of precipitated aragonites may be used as a potential proxy for paleotemperatures if the composition of the primary solution is known and a formation of additional barium containing solids can be excluded.

As the formation of aragonite is triggered by dissolved magnesium ions, co-precipitation of barium and strontium occurs at high Mg^{2+} concentrations (0.02 mol kg^{-1}). Although the concentration of dissolved Mg^{2+} is constant during any experimental run and $Mg(OH)_2$ formation is ruled out (see Section 2), the precipitated aragonite contains small proportions of Mg^{2+}. The ionic radii of Mg^{2+} is small versus that of Ca^{2+} and a rhombohedral magnesium carbonate end member is formed where divalent cations are coordinated to six oxygen. Thus, incorporation of Mg^{2+} into orthorhombic aragonite is low. The value of $K_{\mathrm{Mg,a}}$ can be predicted by the assumption of a hypothetical orthorhombic magnesium carbonate end member and its theoretical solubility product according to Eq. (11). Thermodynamic data by Sverjensky and Molling (1992) imply a value of $K_{\mathrm{Mg,a}}$ between 0.0003 and 0.009 at 25 °C. Tables 3 and 4 show that the $[Mg^{2+}]/[Ca^{2+}]$ ratio of the solutions is about 2.0 ± 0.1, whereas the $X_{\mathrm{MgCO_3}}/X_{\mathrm{CaCO_3}}$ ratios are between 0.0003 and 0.006. Although the respective ratios almost lay within the above theoretical range, the Mg^{2+} content of aragonite is highly divergent and does not depend on temperature and on Sr^{2+} or Ba^{2+} incorporation. Thus, Mg^{2+} content of the aragonite might be affected by complex adsorption phenomena onto the aragonite crystal surface during precipitation rather than to well-regulated substitution into the crystal lattice.

Acknowledgements

The authors greatly appreciate the constructive comments by E.H. Oelkers, C.M. Pina and R.A. Wogelius. **[EO]**

References

Bath, G.E., Thorrold, S.R., Jones, C.M., Campana, S.E., McLaren, J.W., Lam, J.W.H., 2000. Strontium and barium uptake in aragonitic otoliths of marine fish. Geochim. Cosmochim. Acta 64 (10), 1705–1714.

Beck, J.W., Edwards, R.L., Ito, E., Taylor, F.W., Recy, J., Rougerie, F., Joannot, P., Henin, C., 1992. Sea-surface temperature from coral skeletal strontium/calcium ratio. Science 257, 644–647.

Berner, R.A., 1966. Chemical diagenesis of some modern carbonate sediments. Am. J. Sci. 264, 1–36.

Böttcher, M.E., 1997. Comments on "Solid solution partitioning of Sr^{2+}, Ba^{2+}, and Cd^{2+} to calcite" by A.J. Tesoriero and J.F. Pankow. Geochim. Cosmochim. Acta 61 (3), 661–662.

Bradley, D.C., Barbour, S.L., Hendry, M.J., 2001. Osmotic flow through a Cretaceous clay in southern Saskatchewan, Canada. Can. Geotech. J. 38, 1025–1033.

Busenberg, E., Plummer, L.N., 1984. The solubility of strontianite ($SrCO_3$) in CO_2-H_2O solutions between 2 and 91 °C, the association constants of $SrHCO_{3\ (aq)}^{+}$ and $SrCO_{3\ (aq)}^{o}$ between 5 and 80 °C, and an evaluation of the thermodynamic properties of $Sr_{(aq)}^{2+}$ and $SrCO_{3\ (cr)}$ at 25 °C and 1 atm total pressure. Geochim. Cosmochim. Acta 48, 2021–2035.

Busenberg, E., Plummer, L.N., 1986. The solubility of $BaCO_{3\ (cr)}$ (witherite) in CO_2-H_2O solutions between 0 and 90 °C, evaluation of the association constants of $BaHCO_{3\ (aq)}^{+}$ and $BaCO_{3\ (aq)}^{o}$ between 5 and 80 °C, and a preliminary evaluation of the thermodynamic properties of $Ba_{(aq)}^{2+}$. Geochim. Cosmochim. Acta 50, 2225–2233.

Casey, W.H., Chai, L., Navrotosky, A., Rock, P.A., 1996. Thermochemistry of mixing [$SrCO_{3(s)}$] and aragonite [$CaCO_{3(s)}$] to form $Ca_xSr_{1-x}CO_{3(s)}$ solid solution. Geochim. Cosmochim. Acta 60, 933–940.

Culkin, F., 1967. The major constituents of seawater. In: Riley, J.P., Skirrow, G. (Eds.), Chemical Oceanography, vol. 1. Academic Press, London, pp. 121–161.

De Villiers, S., Shen, G.T., Nelson, B.K., 1994. The Sr/Ca-temperature relationship in coralline aragonite; influence of variability in (Sr/Ca) (sub seawater) and skeletal growth parameters. Geochim. Cosmochim. Acta 58 (1), 197–208.

De Villiers, S., Nelson, B.K., Chivas, A.R., 1995. Biological controls on coral Sr/Ca and $\delta^{18}O$ reconstructions of sea surface temperatures. Science 269, 1247–1249.

Dietzel, M., Usdowski, E., 1996. Coprecipitation of Ni^{2+}, Co^{2+}, and Mn^{2+} with galena and covellite, and of Sr^{2+} with calcite during crystallization via diffusion of H_2S and CO_2 through polyethylene at 20 °C: power law and Nernst law control of trace element partitioning. Chem. Geol. 131, 55–65.

Fukuoka, M., 1994. Geomembranes to control movement of rain induced landslides. Proc. 5th IGS Conf. Singapore, 505–508.

Harned, H.S., Davis, R., 1943. The ionization constant of carbonic acid in water and the solubility of carbon dioxide in water and aqueous salt solution from 0 to 50 °C. J. Am. Chem. Soc. 65, 2030–2037.

Henisch, H.K., 1970. Crystal Growth in Gels. The Pennsylvania State Univ. Press, University Park, Pennsylvania, p. 111.

Holland, H.D., Borcsik, M., Munoz, J., Oxburgh, U.M., 1963. The co-precipitation of Sr^{2+} with aragonite and of Ca^{2+} with strontianite between 90 and 100 °C. Geochim. Cosmochim. Acta 27, 957–977.

Joschi, M.S., 1960. Precipitation of carbonates from sea water. Prog. Rep. U.S. AEC Contract No. AT(30-1)-2266.

Jost, W., 1972. Diffusion. Basic phenomena and mechanism. Biomembranes 3, 5–35.

Katz, A., Sass, E., Starinsky, A., Holland, H.D., 1972. Strontium behavior in the aragonite–calcite transformation: an experimental study at 40–98 °C. Geochim. Cosmochim. Acta 36, 481–496.

Kharaka, Y.K., Gunter, W.D., Aggarwall, P.K., Perkins, E.H., DeBraal, J.D., 1988. SOLMINEQ88: a computer program for geochemical modeling of water–rock interactions. U.S.G.S. Wat.-Res. Inv. Rep. 88-4227, 208.

Kinsman, D.J.J., Holland, H.D., 1969. The coprecipitation of cations with $CaCO_3$: IV. The coprecipitation of Sr^{2+} with aragonite between 16° and 96°. Geochim. Cosmochim. Acta 33, 1–17.

Kitano, Y., Kanamori, N., Oomori, T., 1971. Measurements of distribution coefficients of strontium and barium carbonates between carbonate precipitate and solution—abnormally high values of distribution coefficients measured at early stages of carbonate formation. Geochem. J. 4, 183–206.

Kitano, Y., Kanamori, N., Tokuyama, A., Comori, T., 1973. Factors controlling the trace-element contents of marine carbonate skeletons. Proc. Symp. Hydrogeochem. Biochem. I, 484–499.

Lea, D.W., Mashiotta, T.A., Spero, H.J., 1999. Controls on magnesium and strontium uptake in planktonic foraminifera determined by live culturing. Geochim. Cosmochim. Acta 63 (16), 2369–2379.

Lorens, R.B., 1981. Sr, Cd, Mn and Co distribution coefficients in calcite as a function of precipitation rate. Geochim. Cosmochim. Acta 45, 553–561.

McBride, M.B., 1994. Environmental chemistry of soils. Oxford Univ. Press, New York. 406 pp.

Morse, J.W., Mackenzie, F.T., 1990. Geochemistry of sedimentary carbonates. Dev. Sedimentol. 48, 707.

Mucci, A., Morse, J.W., 1983. The incorporation of Mg^{2+} and Sr^{2+} into calcite overgrowths: influences of growth rate and solution composition. Geochimica Cosmochimica Acta 47, 217–233.

Pingitore, N., 1986. Modes of coprecipitation of Ba^{2+} and Sr^{2+} with calcite. In: Davis, J.A., Hayes, K.F. (Eds.), Geochemical Processes at Mineral Surfaces. ACS Symp. Ser., vol. 323, pp. 574–586.

Pingitore, N.E., Eastman, M.P., 1986. The coprecipitation of Sr^{2+} with calcite at 25 °C and 1 atm. Geochim. Cosmochim. Acta 50, 2195–2203.

Plummer, L.N., Busenberg, E., 1982. The solubilities of calcite, aragonite, and vaterite in CO_2-H_2O solutions between 0 and 90 °C and an evaluation of the aqueous model for the system $CaCO_3-CO_2-H_2O$. Geochim. Cosmochim. Acta 46, 1011–1040.

Plummer, L.N., Busenberg, E., 1987. Thermodynamics of aragonite–strontianite solid solutions: results from stoichiometric solubility at 25 and 76 °C. Geochim. Cosmochim. Acta 51, 1393–1411.

Plummer, L.N., Busenberg, E., Glynn, P.D., Blum, A.E., 1992.

Dissolution of aragonite–strontianite solid solutions in nonstoichiometric $Sr(HCO_3)_2$–$Ca(HCO_3)_2$–CO_2–H_2O solutions. Geochim. Cosmochim. Acta 56, 3045–3072.

Prieto, M., Fernandez-Gonzalez, A., Putnis, A., Fernandez-Diaz, L., 1997. Nucleation, growth, and zoning phenomena in crystallizing $(Ba,Sr)CO_3$, $Ba(SO_4,CrO_4)$, $(Ba,Sr)SO_4$, and $(Cd,Ca)CO_3$ solid solutions from aqueous solutions. Geochim. Cosmochim. Acta 61 (16), 3383–3397.

Rickaby, R.E.M., Schrag, D.P., 2002. Growth rate dependence of Sr incorporation during the calcification of *Emiliania huxleyi*. Global Biochem. Cycle 16 (1), 1–8.

Rimstidt, J.D., Balog, A., Webb, J., 1998. Distribution of trace elements between carbonate minerals and aqueous solutions. Geochim. Cosmochim. Acta 62 (11), 1851–1863.

Smith, S.V., Buddemeier, R.W., Redaije, R.C., Houck, J.E., 1979. Strontium–calcium thermometry in coral skeletons. Science 204, 404–407.

Sverjensky, D.A., Molling, P.A., 1992. A linear free energy relationship for crystalline solids and aqueous ions. Nature 356, 231–234.

Tesoriero, A.J., Pankow, J.F., 1996. Solid solution partitioning of Sr^{2+}, Ba^{2+}, and Cd^{2+} to calcite. Geochim. Cosmochim. Acta 60 (6), 1053–1063.

Unger, S.L., 1984. Fabrication of Welded Polyethylene Encapsulates to Secure Drums Containing Hazardous Wastes, Proc. Land Disposal of Hazardous Waste, EPA-600/9-84-007, April, pp. 78–89

Unver, A.A., Himmelblau, D.M., 1964. Diffusion coefficients of CO_2, C_2H_4, C_3H_6, and C_4H_8 in water from 6° to 65 °C. J. Chem. Eng. Data 9 (3), 428–431.

Usdowski, E., 1973. Das geochemische Verhalten des Strontiums bei der Genese und Diagenese von Ca-Karbonat und Ca-Sulfat-Mineralen. Contrib. Mineral. Petrol. 38, 177–195.

Weber, J.N., 1973. Incorporation of strontium into reef corals skeletal carbonate. Geochim. Cosmochim. Acta 37 (9), 2173–2191.

Zhou, G.-T., Zheng, Y.-F., 2001. Chemical synthesis of $CaCO_3$ minerals at low temperatures and implication for mechanism of polymorphic transition. Neues Jahrb. Mineral. Abh. 176 (3), 323–343.